Water Environment Federation
the water quality people™

Three-dimensional carbon-based anodes promoted the accumulation of exoelectrogens in bioelectrochemical systems

Yicheng Wu ,[1,2] Guanghua He ,[2,3] Shuiliang Chen ,[2,3] Zejie Wang [2,4,*]

[1] Fujian Engineering and Research Center of Rural Sewage Treatment and Water Safety, Xiamen University of Technology, Xiamen, China

[2] Key Laboratory of Urban Pollutant Conversion, Institute of Urban Environment, Chinese Academy of Sciences, Xiamen, China

[3] Department of Chemistry and Chemical Engineering, Jiangxi Normal University, Nanchang, China

[4] College of Environmental Science and Engineering, Qilu University of Technology (Shandong Academy of Sciences), Jinan, China

Received 8 October 2019; Revised 17 December 2019; Accepted 24 December 2019

Natural Science Foundation of Fujian Province, Grant/Award Number: 2019J01848; Xiamen University of Technology, Grant/Award Number: XPDKQ18032; Xiamen Municipal Bureau of Science and Technology, Grant/Award Number: 3502Z20179029

Additional Supporting Information may be found in the online version of this article.

Correspondence to: Zejie Wang, Key Laboratory of Urban Pollutant Conversion, Institute of Urban Environment, Chinese Academy of Sciences, Xiamen, China. Email: wangzejie@qlu.edu.cn

Y. Wu and G. He are contributed equally to this work.

DOI: 10.1002/wer.1293

Abstract

To achieve deep understandings on the effects of structure and surface properties of anode material on the performance of bioelectrochemical systems, the present research investigated the bacterial community structures of biofilms attached to different three-dimensional anodes including carbon felt and materials derived from pomelo peel, kenaf stem, and cardboard with 454 pyrosequencing analysis based on the bacterial 16S rRNA gene. The results showed that bacterial community structures, especially the relative abundance of exoelectrogens, were significantly related to the types of adopted three-dimensional anode materials. Proteobacteria was the shared predominant phylum, accounting for 55.4%, 52.1%, 66.7%, and 56.1% for carbon felt, cardboard, pomelo peel, and kenaf stem carbon, respectively. The most abundant OTU was phylogenetically related to the well-known exoelectrogen of *Geobacter*, with a relative abundance of 16.3%, 19.0%, 36.3%, and 28.6% in carbon felt, cardboard, pomelo peel, and kenaf stem, respectively. Moreover, another exoelectrogen of *Pseudomonas* sp. accounted for 4.9% in kenaf stem and 3.9% in carbonboard, respectively. The results implied the macrostructure and properties of different anode materials might result in different niches such as hydrodynamics and substrate transport dynamics, leading to different bacterial structure, especially different relative abundance of exoelectrogens, which consequently affected the performance of bioelectrochemical systems. © 2019 Water Environment Federation

Practitioner points

- Bioelectrochemical systems (BESs) represent a novel biotechnology platform to simultaneously treat wastewaters and produce electrical power.
- Three-dimensional materials derived from nature plant as anode to promote electricity output from BESs and reduce the construct cost of BESs.
- Macrostructure of the three-dimensional anode material affected phylotype richness and phylogenetic diversity of microorganisms in anodic biofilm of BESs.
- *Geobacter* as well-known exoelectrogen was the most abundant in biofilm attached to three-dimensional anode.

Key words

454 pyrosequencing; bioelectrochemical systems; biofilm; carbonized natural material; microbial community structure

Introduction

Bioelectrochemical systems (BESs) represent a novel biotechnology platform to simultaneous treat wastewaters and produce electrical power with the aid of exoelectrogens (Huang, Chai, Chen, & Logan, 2011; Liu, Grot, & Logan, 2005; Xiao, Zheng, Wu, Yang, & Zhao, 2016). Over traditional biotechnology, BESs take the advantages of low-consumption of energy, high-efficiency of pollutant removal, conversion of

wastes to energy, and less-production of sludge. Therefore, BESs attract increasing attentions world widely from the perspectives of electrochemistry, materials, microbiology, and engineering (Cao et al., 2009; Wang, Liu, & Sun, 2010; Wang, Feng, et al., 2010; Zhan et al., 2012).

Electric power is the primary energy output from BESs. And thus, many efforts were made to promote the electric power generation (Daniele, Silvia, Daniele, Arianna, & Andrea, 2018; Kundu, Bergmann, Klocke, Sharma, & Sreekrishnan, 2014; Song et al., 2015). The characteristics of anode materials were verified as important factors affecting the electric power output from BESs (Vila Rovira, Puig Broch, Dolors, & Colprim, 2015). Two-dimensional materials were firstly used to set up BESs. However, the electric power density from BESs with two-dimensional anode was not satisfactory.

Three-dimensional (3D) materials like textile (Wang, Liu, et al., 2010; Wang, Feng, et al., 2010), graphite felt (Wang, Liu, et al., 2010; Wang, Feng, et al., 2010), bread (Zhang, He, et al., 2018; Zhang, Chen, et al., 2018), graphite aerogel (Zhao et al., 2015), carbon foam (Han, Sawant, Hwang, & Cho, 2016), and biomass such as corn stem (Karthikeyan et al., 2015), pomelo peel (Chen, He, Hu, et al., 2012), kenaf stems (Chen, He, Liu, et al., 2012), and cardboard (Chen, Liu, et al., 2012) as anode substrate were observed effective to promote electric power output from BESs, because that their special macrostructures benefited for the formation of biofilm and substrate diffusion (Wang, Liu, et al., 2010; Wang, Feng, et al., 2010). For the better performance of 3D anodes, prior researches provided explanations from the perspectives of materials' properties, biofilm morphology, and bio-electrochemistry (Chen, He, Hu, et al., 2012; Wang, Liu, et al., 2010; Wang, Feng, et al., 2010). However, theses explanations could not provide comprehensive understandings on the better performance of 3D anodes, because that bacterium, especially exoelectrogens, plays key role in the electric power generation (Lovley, 2006). Other bacteria than exoelectrogens could create an optimal niche to support the exoelectrogens to perform better functions of electron transfer, for example, aerobic bacteria could consume dissolved oxygen to form anaerobic circumstances for exoelectrogens. Therefore, analysis of bacteria community deserves great significance to comprehensively understand the better performance of 3D anodes.

The present research selected three types of 3D materials derived from pomelo peel (Chen, He, Hu, et al., 2012), kenaf stems (Chen, He, Liu, et al., 2012), and cardboard (Chen, Liu, et al., 2012), and graphite as a control. Biofilm samples were collected from the anodes and further microbial community structures were revealed with the aid of 454 pyrosequencing (Figure 1). Together with the characteristics of the anodes, the present research demonstrated the insights on the better performance of 3D anodes from the perspectives of anodic microbiology.

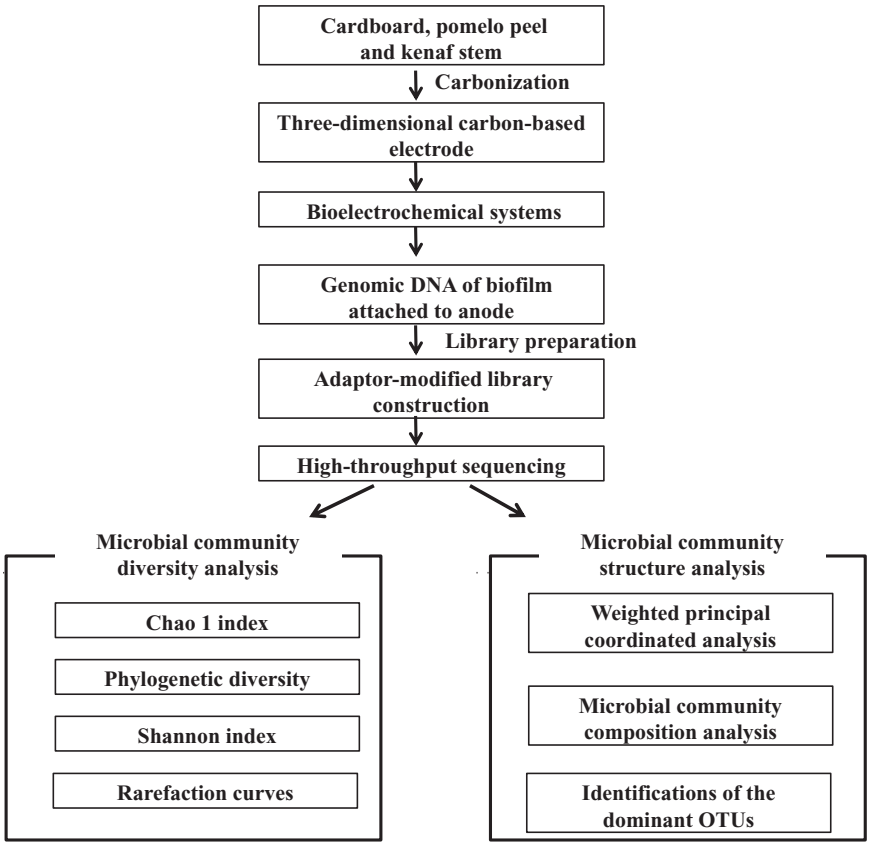

Figure 1. Workflow of microbial community structure analysis of biofilm attached to three-dimensional carbon-based electrode.

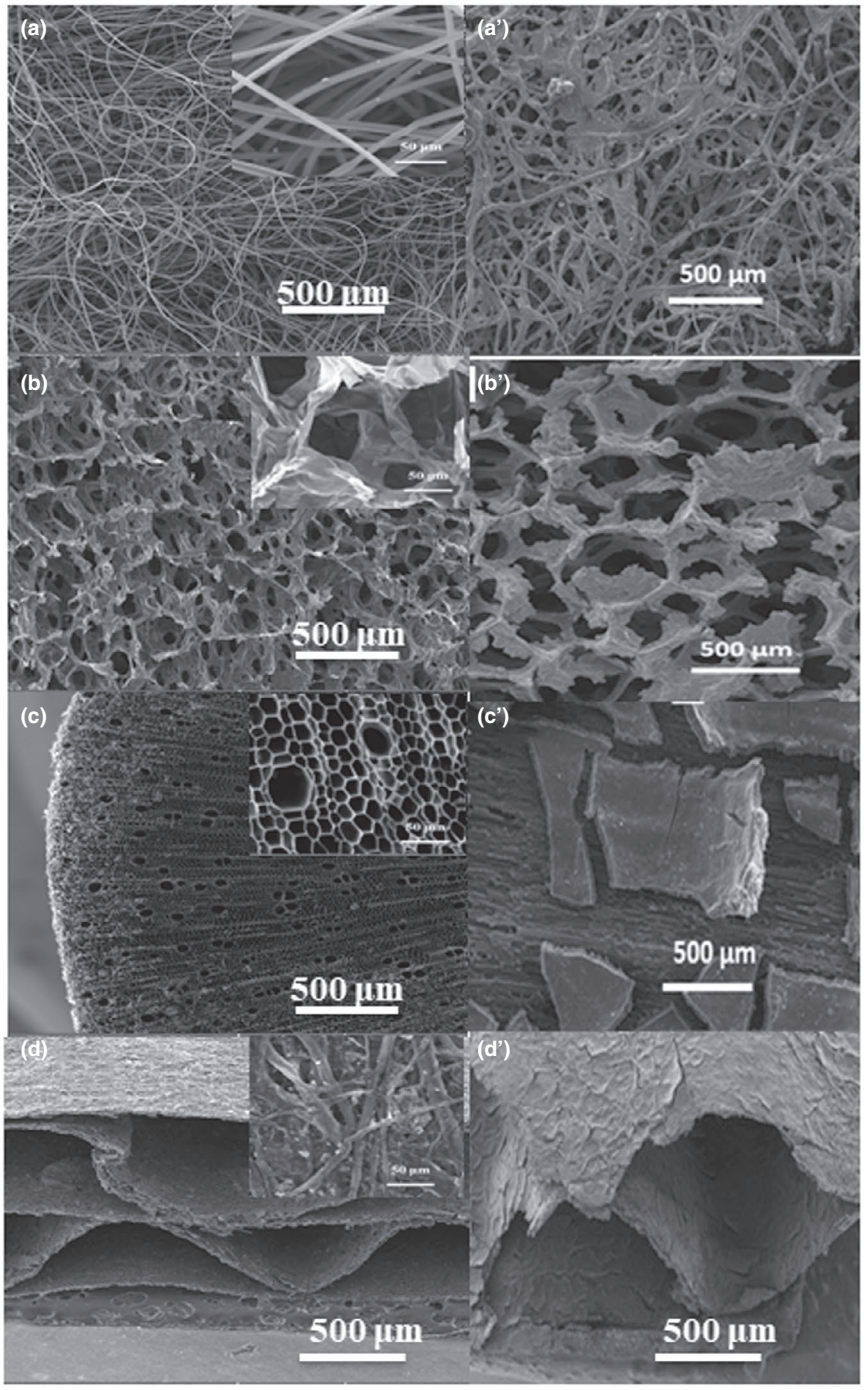

Figure 2. SEM images of different magnifications of three-dimensional carbon-based electrodes and the attached biofilm. Images (a), (b), (c), and (d) are carbonized carbon felt, pomelo peel, kenaf stem, and cardboard, respectively. And images (a'), (b'), (c'), and (d') are biofilm attached to carbonized carbon felt, pomelo peel, kenaf stem, and cardboard, respectively.

Methods and Materials

Samples

The electrode preparation and reactor setup were descripted in our previous researches (Chen, He, Hu, et al., 2012; Chen, He, Liu, et al., 2012; Chen, Liu, et al., 2012). The samples of anodic biofilm were collected from the four anodes made of carbon felt (CF), carbonized pomelo peel (PP), kenaf stem (KS), and cardboard (CB).

DNA extraction

The collected biofilm was gently rinsed with deionized water to remove loosely attached microbes and then fragmented using sterile scissors. Genomic DNA was extracted using a Power Soil

Table 1. Pyrosequencing information of CF, CB, PP, and KS

	3% DISTANCE					
SAMPLE	EFFECTIVE SEQUENCES	OTUS	CHAO 1	PHYLOGENETIC DIVERSITY	SHANNON INDEX	COVERAGE (%)
CF	11,941	3,413	14,248	219.39	8.57	77.62
CB	11,836	28,213	13,153	188.60	7.89	81.31
PP	11,743	2,768	11,694	187.51	7.03	82.01
KS	8,920	2,212	9,929	155.68	7.28	80.43

DNA isolation kit (MO BIO Laboratories, USA) and purified with a kit (Cat. # DP1501; BioTeke, China) according to the instructions. The quality and quantity of the extracted DNA were assessed by agarose gel electrophoresis and absorbance measurements at 260 and 280 nm using a ND-2000 spectrophotometer (Nanodrop Inc., USA).

High-throughput pyrosequencing

The primer 27F (5′-AGAGTTTGATCCTGGCTCAG-3′) and 533R (5′-TTACCGCGGCTGCTGGCAC-3′) were used in the amplification of the V3 region of the bacterial 16S r RNA gene. Each sample was amplified following our previous study (Wang et al., 2013). The amplification products were quantitated by QuantiFluor™-ST and then mixed for high-throughput sequencing.

Biodiversity analysis and phylogenetic classification

Low-quality sequences were removed by the Quantitative Insights into microbial ecology (QIIME, version 1.6) software. In addition, sequences were clustered into operational taxonomic units (OTUs) by setting a 0.03 distance limit. Hierarchical cluster analysis and weighted principal coordinated analysis (PCA) were conducted using MOTHUR (Schloss et al., 2009). The number of OTUs, Chao1 index, and phylogenetic richness index diversity were calculated to estimate diversity and richness of each sample.

Results

Amorphous morphology of anode

The surface morphology and structure of the 3D anode materials and attached biofilm were observed with scanning electron microscopy (SEM). It was demonstrated that the 3D materials showed completely different structures. CF was comprised of microfibers with a smooth surface, forming loose aggregates (Figure 2a). After carbonization, the PP formed a carbon networks, with a wrinkled surface and pore size of over 100 μm (Figure 2b). However, the carbonized KS material was composed of hexagonal macro-channels, with a diameter of ca. 25 μm or ca. 60 μm. The macro-channels uniformly distributed in the materials (Figure 2c). The CB has a rough surface and corrugated carbon skeleton with a wavelength of about 1,000 μm, which retains the original macro-channel layered structure (Figure 2d). SEM images (a'), (b'), (c'), and (d') show that thick biofilms were grown on the surface of the anodes. For carbonized anodes, however, plenty of micropores were left, which was beneficial for the mass transfer and further the performance of electroactive biofilm. The full-scan XPS spectra analysis in Supporting Information Figure S1 shows that CB, KS, and PP were rich in heteroatoms, such as O, S, and P, which might be beneficial for the growth of bacteria.

Richness and diversity of phylotypes

A total of 44,440 16S rDNA sequencing reads (11,941 for CF, 11,836 for CB, 11,743 for PP and 8,920 for KS) were produced by Roche GS FLX PLUS System following the sequence quality filtering steps. The number of obtained OTUs was 3,413, 2,821, 2,768, and 2,212 for CF, CB, PP, and KS, respectively (Table 1). Chao1 estimation suggested that bacterial community in CF was more diverse than those in other samples, which was further confirmed by the richness parameters such as Shannon index and phylogenetic diversity. The rarefaction curves exhibited an increasing trend even when sequencing reads were close to or more than 10,000, implying the emergence of new microbial phylotypes (Figure 3).

Comparative analysis of microbial community

Hierarchical cluster analysis and weighted PCA were used to identify the differences of the four bacterial community structures. As shown in Figure 4, there were two clusters in hierarchical cluster analysis, CF and CB were separated from PP and KS, suggesting clear distinctions of bacterial community structure between the anodic biofilms despite they inoculated the same sludge. It was further confirmed

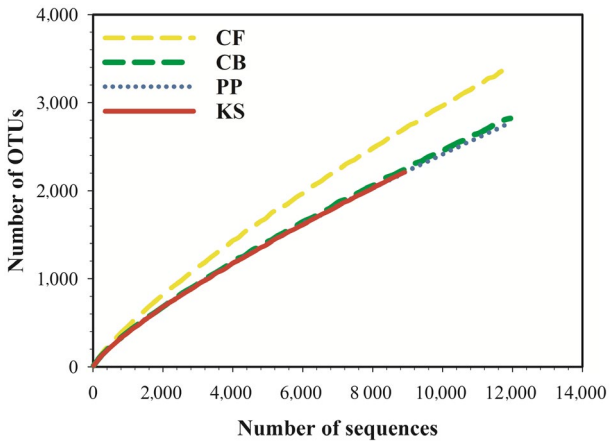

Figure 3. Rarefaction curves based on pyrosequencing of CF, CB, PP and KS. The OTUs were defined by 3% distance.

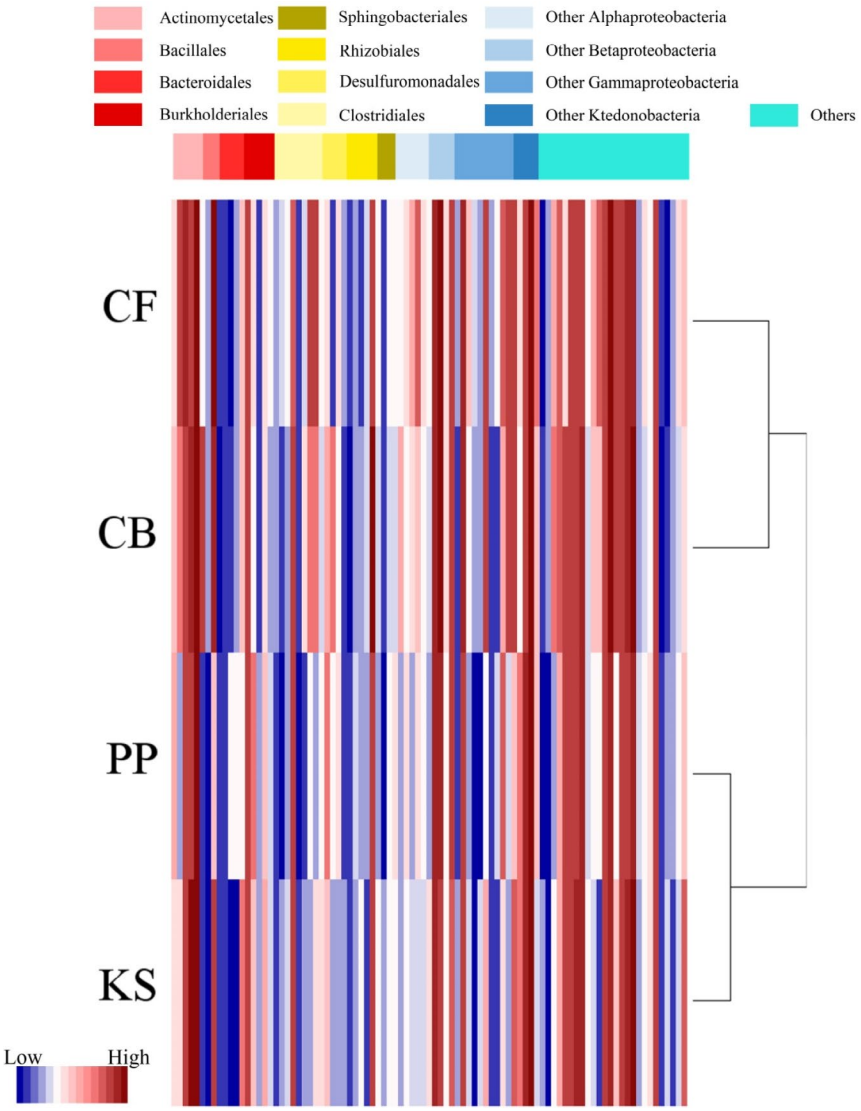

Figure 4. Hierarchical cluster analysis of CF, CB, PP, and KS bacterial communities. The OTUs were ordered by class. Sample communities were clustered based on complete linkage method. The color intensity of scale indicates relative abundance of each OUT read. Relative abundance was defined as the number of sequences affiliated with that OTU divided by the total number of sequences per sample.

by weighted PCA, for which The CF and CB were clustered together, while KS and PP were closer (Figure 5). The CF and CB demonstrated larger space compared to KS and PP, which would be beneficial for the mass transport. That might be reason for the close clustering of bacterial community of CF and CB, KS, and PP.

Distribution of phylotypes

To compare the distribution of phylotypes in CF, CB, PP, and KS, the qualified reads were assigned to known taxonomies at phylum, class, and order level (Figure 6). At the level of phylum, there were seven dominant bacterial phyla (relative abundance > 1.8%). Proteobacteria was the shared dominant phylum in the samples, accounting for 66.7% in PP, 56.1% in KS, 55.4% in CF, and 52.1% in CB, respectively. Bacteroidetes (6.3%–15.8%) and Firmicutes (8.7%–9.2%) were sub-dominant phyla. The three phyla accounted for 80.0%, 76.9%, 81.7%, and 78.3% for CF, CB, PP, and KS respectively. The results were consistent with the study of Koch and Harnisch (2016), which showed that exoelectrogenic are mainly distributed in several phylotypes such as Proteobacteria and Firmicutes.

At the level of class, there were ten dominant bacterial classes (relative abundance > 1.4%, Figure 7). *Deltaproteobacteria* from the phylum of Proteobacteria was the most dominant class in all the biofilm samples, with a relative abundance of 49.4% in PP, 39.6% in KS, 27.6% in CB, and 25.8% in CF, respectively. It was reported that *Deltaproteobacteria* was detectable at a high frequency of 50%–91% in the anodic community of MFCs, probably due to that it favorites the stress of electric current generation (Yokoyama, Ishida, & Yamashita, 2016). *Betaproteobacteria* was

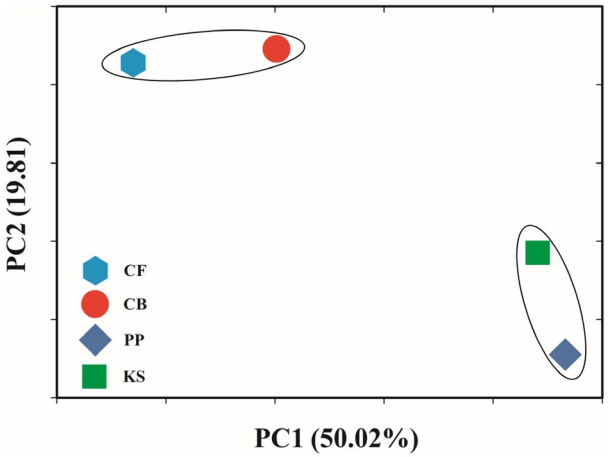

Figure 5. Weighted principal coordinated analysis of bacterial communities of CF, CB, PP, and KS using the UniFran matrix.

the sub-dominant class for CF (6.2%) and CB (6.3%), while *Bacteroidia* as the sub-dominant class for PP (2.9%) and KS (6.1%). *Desulfuromonadales* was the most dominant order in the samples, accounted for 47.7% in PP, relative to 25.7%, 24.4%, and 37.5%, for CB, CF, and KS, respectively.

Characterization of dominant OTUs

A total of 11,214 OTUs were generated for the samples from the high-throughput sequencing results (Table 1). Among them, 468 OTUs were shared by the four samples. Moreover, 23 OTUs were determined with a relative abundance higher than 0.5%, accounting for 42.5%–53.9% of the total sequences. There were 2, 4, 4, and 5 out of the 23 OTUs belonging to the classes of *alpha-*, *Beta-*, and *Deltaproteobacteria*, and *Bacteroidia*, respectively, while *Spirochaetes*, *Holophagae*, and *Endomicrobia* contained only one OTU in each sample.

The relative abundance and identification of the dominant OTUs according to the results of BLAST were illustrated in Figure 8. There were 20 GenBank matches belonging to cultured bacteria, and the other three OTUs were unclassified. The relative abundance of each OTU in CF, CB, PP, and KS was different. Among these 23 dominant OTUs, there were three OTUs (1858, 2272, and 9058) with a relative abundance higher than 3.5% in CB, and two OTUs in CF (41 and 2272) and KS (1858 and 2272), while only one OTU (2272) in PP. The results indicated that only a few microbial species dominated in the biofilms despite of the high diversity in the communities. OTU-2272 was the most abundant OTU in all samples, accounting for 16.3%, 19.0%, 36.3%, and 28.6% in CF, CB, PP, and KS, respectively. OTU-2272 was phylogenetically related (99% identity) to *Geobacter* according to the result of BLAST. *Geobacter* was one of the most widely reported exoelectrogen (Lovley, 2012). *Geobacter* spp. could produce and transfer electrons through highly conductive pili, enabling efficient transfer of electrons to the anode (Logan, Rossi, Ragab, & Saikaly, 2019). OUT-1858 was 99% identical to *Pseudomonas* sp., an exoelectrogen with self-secreted pyocyanin as electron shuttle (Rabaey, Boon, Siciliano, Verhaege, & Verstraete, 2004). It accounted for 4.9% in KS and 3.9% in CB. The results indicated that the anode made of carbonized natural materials had good selective effect to exoelectrogens. OTU-1858 and OTU-2272 had a total relative abundance of 17.3%, 22.8%, 37.9%, and 33.5% in CF,

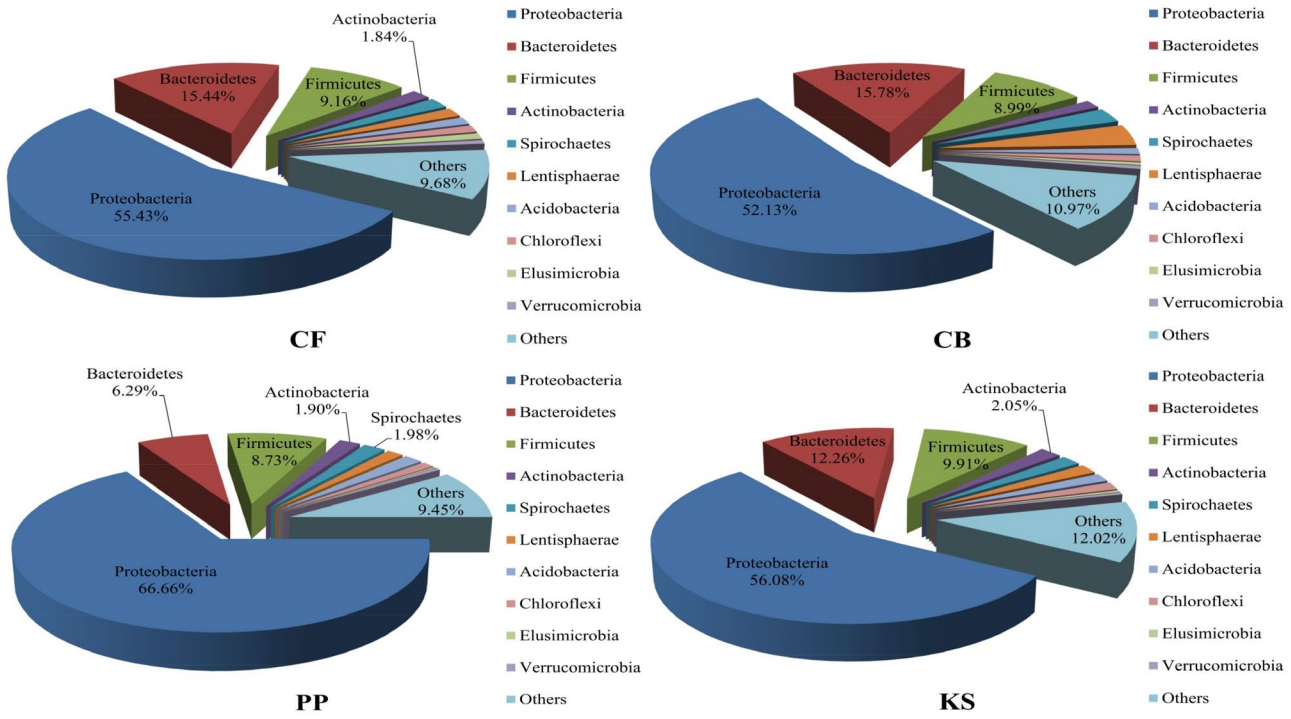

Figure 6. Relative abundance of microbial community composition at phylum levels in CF, CB, PP, and KS.

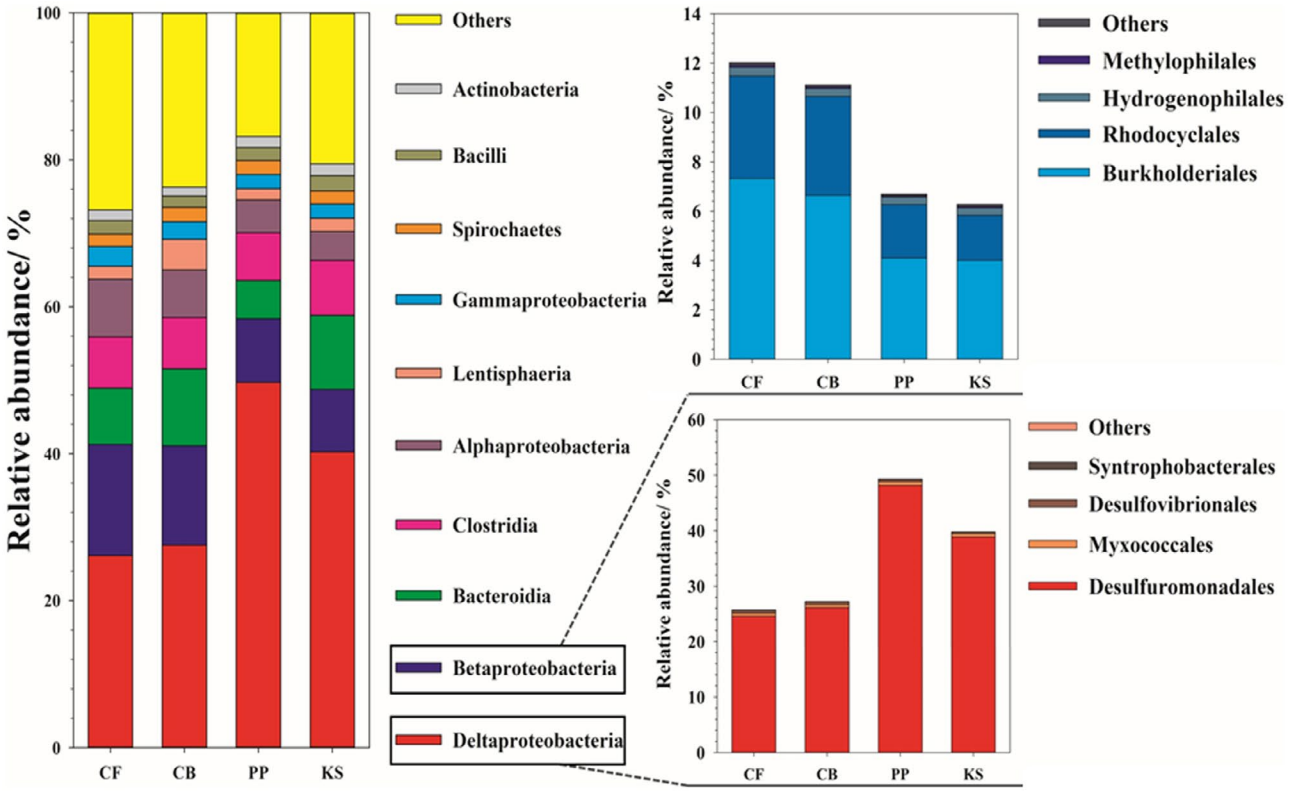

Figure 7. Relative abundance of microbial community composition at class and order levels in CF, CB, PP and KS.

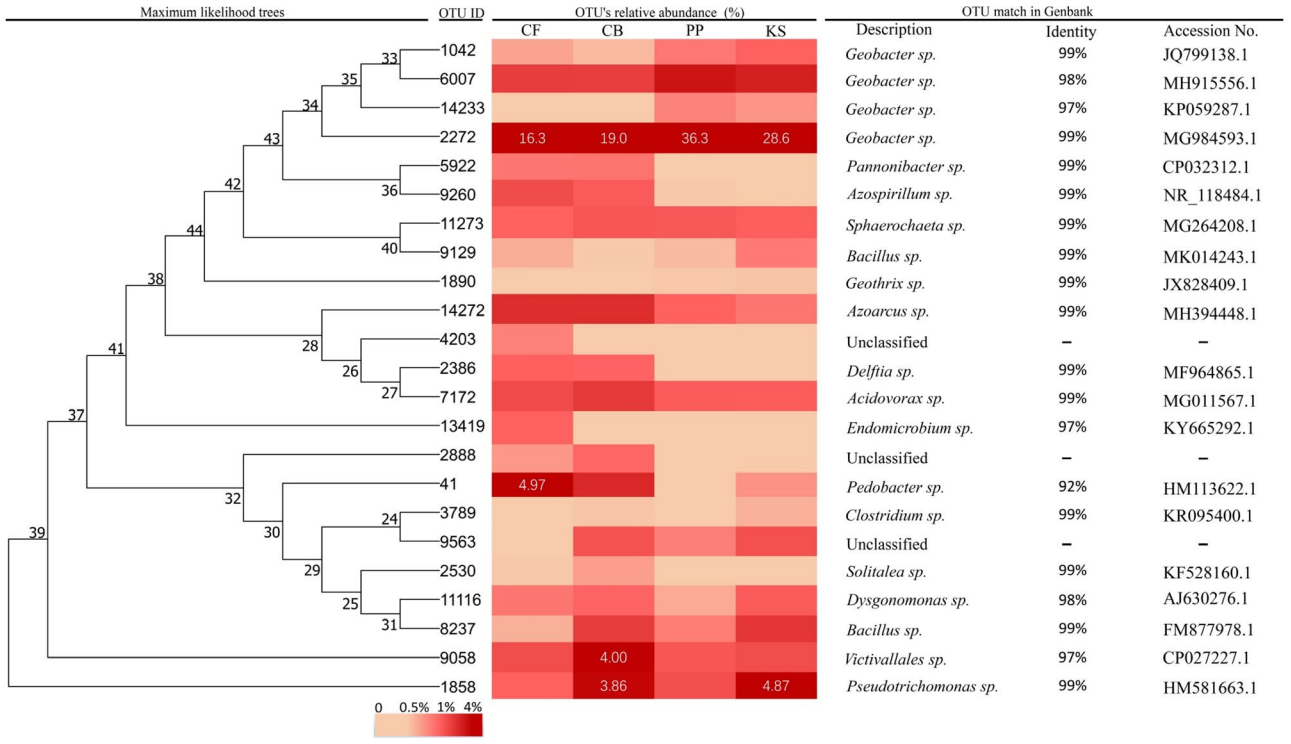

Figure 8. Relative abundances and identifications of the dominant OTUs in CF, CB, PP, and KS. The color intensity in each panel shows the relative abundance (in percentage) of a genus in a sample, referring to color key at the right top.

CB, PP, and KS, respectively. They were responsible for the electric current generation. And thus, it could be concluded that the novel materials selected more exoelectrogens and output more electric power. However, BES with carbonized CB as anode generated more electricity than that of carbonized PP as anode under the same condition although there was more electrochemically active microorganism in PP. The result indicated that the relative abundance of exoelectrogens was a key, but not the sole factor to affect the electrochemical performance of the biofilm anode.

Discussion

The performance of BESs with the selected anode materials has been showed in our prior researches (Chen, He, Hu, et al., 2012; Chen, He, Liu, et al., 2012; Chen, Liu, et al., 2012). In brief, the 3D anode prepared from KS generated a maximum current density of 32.5 A/m^2, compared to 40 A/m^2 from PP, which was 2.5 times that of graphite felts. The maximum current density from corrugated CB anode was 2 times higher than that from KS. The structure of anode materials could affect the growth of microorganisms, while the properties of materials could affect the microbial composition. Three kinds of three-dimensional carbon-based anodes derived from natural plant are different in their structure (Figure 2). Moreover, the porous carbon materials derived from natural plants were rich in heteroatoms, such as O, S, and P, which would enhance their hydrophilicity and thus facilitated the growth of microorganisms in biofilm attached to anode (Supporting Information Table S1). Moreover, the different macrostructure of the anode materials would affect the mass transport and electron transfer efficiency (Gilberto, Filipa, Luciana, & Madalena, 2018).

Many attentions were paid to the distribution of community structure of biofilms in BES. It was observed that the bacterial community structure was related to several factors such as substrate (Zhang, Min, Huang, & Angelidaki, 2011), external resistance (de Cárcer, Phuc, Jang, & Chang, 2011), and electric current density (Cai, Zheng, Xing, & Qaisar, 2015). The properties of anode should be important factors to the bacterial community structure because that the biofilm attached tightly to the surface of anode. Zhang et al. (2018) evaluated the effects of carbon nanotube on the long-term performance and microbial community structure of graphite anode in microbial fuel cells. It was observed that the modification of graphite anode with carbon nanotube increased the relative abundance of *Geobacter* species which further enhanced the power generation and long-term stability. In the present research, the different anode possessed different properties, which further affected the bacterial community structures, especially the accumulation of exoelectrogens. Proteobacteria, Bacteroidetes, and Firmicutes were observed dominant in the biofilms collected from the surface of CF, CB, PP, and KS. They were often detected as dominant phylum in the electroactive biofilms, for example, these on the anode surface of carbon felt and graphite fiber brush (Wu, Zheng, Xiao, Wang, & Zhao, 2017; Xiao, Wu, & Yang, 2013; Yates et al., 2012; Zhao et al., 2019), probably because that they could well adopt the drive force of electron transfer. And thus, they were widely known source of exoelectrogens (Wang, Liu, et al., 2010; Xiao et al., 2013).

Desulfuromonadales was the most dominant order in the samples. There are many exoelectrogens such as *Desulfuromonas acetoxidans*, *Desulfovibrio desulfuricans*, *Geobacter sulfurreducens*, and *Geopsychrobacter electrodiphilus* belonging to *Desulfuromonadales* (Bond, Holmes, & Tender, 2002; Bond & Lovley, 2003; Zhao et al., 2008). Among them, *G. sulfurreducens* is the first reported microorganism with anode as the final electron acceptor under anaerobic conditions (Bond et al., 2002).

Conclusions

The present research revealed that the surface properties and macrostructure of the 3D anode material affected the phylotype richness and phylogenetic diversity of microorganisms in anodic biofilm of BESs. Similar macrostructure resulted in closer cluster of bacterial community structure. The content of exoelectrogens such as *Geobacter* and *Pseudomonas* in biofilms attached to the anodes made of different natural materials was greatly increased. And thus, such 3D materials promoted the electric power generation compared to conventional materials such as graphite felt. However, the relative abundance of exoelectrogens was not the sole factor to the performance of BESs. These results further clarified how anode material affected the bacterial communities, which consequently affected the performance of BESs.

Acknowledgments

This work was supported by Natural Science Foundation of Fujian Province (2019J01848), Xiamen Science and Technology Plan Guidance Project (3502Z20179029), and Scientific Climbing Plan of Xiamen University of Technology (XPDKQ18032).

References

Bond, D. R., Holmes, D. E., & Tender, L. M. (2002). Electrode-reducing microorganisms that harvest energy from marine sediments. *Science*, *295*, 483–485. https://doi.org/10.1126/science.1066771

Bond, D. R., & Lovley, D. R. (2003). Electricity production by *Geobacter sulfurreducens* attached to electrodes. *Applied and Environmental Microbiology*, *69*, 1548–1555. https://doi.org/10.1128/AEM.69.3.1548-1555.2003

Cai, J., Zheng, P., Xing, Y. J., & Qaisar, M. (2015). Effect of electricity on microbial community of microbial fuel cell simultaneously treating sulfide and nitrate. *Journal of Power Sources*, *281*, 27–33. https://doi.org/10.1016/j.jpowsour.2015.01.165

Cao, X., Huang, X., Liang, P., Xiao, K., Zhou, Y., Zhang, X., & Logan, B. E. (2009). A new method for water desalination using microbial desalination cells. *Environmental Science and Technology*, *43*, 7148–7152. https://doi.org/10.1021/es901950j

Cárcer, D. A., Phuc, T. H., Jang, J. K., & Chang, I. S. (2011). Microbial community differences between propionate-fed microbial fuel cell systems under open and closed circuit conditions. *Applied Microbiology and Biotechnology*, *89*, 605–612. https://doi.org/10.1007/s00253-010-2903-x

Chen, S., He, G., Hu, X., Xie, M., Wang, S., Zeng, D., … Schröder, U. (2012). A three-dimensionally ordered macroporous carbon derived from a natural resource as anode for microbial bioelectrochemical systems. *Chemsuschem*, *5*, 1059–1063. https://doi.org/10.1002/cssc.201100783

Chen, S., He, G., Liu, Q., Harnisch, F., Zhou, Y., Chen, Y. U., … Schröder, U. (2012). Layered corrugated electrode macrostructures boost microbial bioelectrocatalysis. *Energy and Environmental Science*, *5*, 9769–9772. https://doi.org/10.1039/c2ee23344d

Chen, S., Liu, Q., He, G., Zhou, Y., Hanif, M., Peng, X., … Hou, H. (2012). Reticulated carbon foam derived from a sponge-like natural product as a high-performance anode

in microbial fuel cells. *Journal of Materials Chemistry*, *22*, 18609–18613. https://doi.org/10.1039/c2jm33733a

Daniele, C., Silvia, B., Daniele, M., Arianna, C., & Andrea, G. (2018). Influence of reactor's hydrodynamics on the performance of microbial fuel cells. *Journal of Water Process Engineering*, *26*, 281–288.

Gilberto, M., Filipa, S. A., Luciana, P., & Madalena, A. M. (2018). Methane production and conductive materials: A critical review. *Environmental Science Technology*, *52*, 10241–10253. https://doi.org/10.1021/acs.est.8b01913

Han, T. H., Sawant, S. Y., Hwang, S. J., & Cho, M. H. (2016). Three-dimensional, highly porous N-doped carbon foam as microorganism propitious, efficient anode for high performance microbial fuel cell. *RSC Advances*, *6*, 25799–25807. https://doi.org/10.1039/C6RA01842D

Huang, L., Chai, X., Chen, G., & Logan, B. E. (2011). Effect of set potential on hexavalent chromium reduction and electricity generation from biocathode microbial fuel cells. *Environmental Science and Technology*, *45*, 5025–5031. https://doi.org/10.1021/es103875d

Karthikeyan, R., Wang, B., Xuan, J., Wong, J. W. C., Lee, P. K. H., & Leung, M. K. H. (2015). Interfacial electron transfer and bioelectrocatalysis of carbonized plant material as effective anode of microbial fuel cell. *Electrochimica Acta*, *157*, 314–323. https://doi.org/10.1016/j.electacta.2015.01.029

Koch, C., & Harnisch, F. (2016). Is there a specific ecological niche for electroactive microorganisms? *ChemElectroChem*, *3*, 1282–1295. https://doi.org/10.1002/celc.201600079

Kundu, K., Bergmann, I., Klocke, M., Sharma, S., & Sreekrishnan, T. R. (2014). Influence of hydrodynamic shear on performance and microbial community structure of a hybrid anaerobic reactor. *Journal of Chemical Technology and Biotechnology*, *89*(3), 462–470. https://doi.org/10.1002/jctb.4194

Liu, H., Grot, S., & Logan, B. E. (2005). Electrochemically assisted microbial production of hydrogen from acetate. *Environmental Science and Technology*, *39*, 4317–4320. https://doi.org/10.1021/es050244p

Logan, B. E., Rossi, R., Ragab, A., & Saikaly, P. E. (2019). Electroactive microorganisms in bioelectrochemical systems. *Nature Reviews Microbiology*, *17*, 307–319. https://doi.org/10.1038/s41579-019-0173-x

Lovley, D. R. (2006). Bug juice: Harvesting electricity with microorganisms. *Nature Reviews Microbiology*, *4*, 497. https://doi.org/10.1038/nrmicro1442

Lovley, D. R. (2012). Electromicrobiology. *Annual Review of Microbiology*, *66*, 391. https://doi.org/10.1146/annurev-micro-092611-150104

Rabaey, K., Boon, N., Siciliano, S. D., Verhaege, M., & Verstraete, W. (2004). Biofuel cells select for microbial consortia that self-mediate electron transfer. *Applied and Environmental Microbiology*, *70*, 5373–5382. https://doi.org/10.1128/AEM.70.9.5373-5382.2004

Schloss, P. D., Westcott, S. L., Ryabin, T., Hall, J. R., Hartmann, M., Hollister, E. B., … Weber, C. F. (2009). Introducing mothur: Open-Source, platform-independent, community-supported software for describing and comparing microbial communities. *Applied Environmental Microbiology*, *75*, 7537–7542. https://doi.org/10.1128/AEM.01541-09

Song, Y. C., Kim, D. S., Woo, J. H., Subha, B., Jang, S. H., & Sivakumar, S. (2015). Effect of surface modification of anode with surfactant on the performance of microbial fuel cell. *International Journal of Energy Research*, *39*(6), 860–868. https://doi.org/10.1002/er.3284

Vila Rovira, A., Puig Broch, S., Dolors, B. I. C. M., & Colprim, G. J. (2015). Anode hydrodynamics in bioelectrochemical systems. *Rsc Advances*, *5*(96), 78994–79000. https://doi.org/10.1039/C5RA11995B

Wang, A., Liu, L., & Sun, D. (2010). Isolation of Fe(III)-reducing fermentative bacterium *Bacteroides* sp. W7 in the anode suspension of a microbial electrolysis cell (MEC). *International Journal of Hydrogen Energy*, *35*, 3178–3182.

Wang, X., Feng, Y., Liu, J., Lee, H., Li, C., Li, N., & Ren, N. (2010). Sequestration of CO_2 discharged from anode by algal cathode in microbial carbon capture cells (MCCs). *Biosensors and Bioelectronics*, *25*, 2639–2643. https://doi.org/10.1016/j.bios.2010.04.036

Wang, Z., Zheng, Y., Xiao, Y., Wu, S., Wu, Y., Yang, Z., & Zhao, F. (2013). Analysis of oxygen reduction and microbial community of air-diffusion biocathode in microbial fuel cells. *Bioresource Technology*, *144*, 74–79. https://doi.org/10.1016/j.biortech.2013.06.093

Wu, Y., Zheng, Y., Xiao, Y., Wang, Z., & Zhao, F. (2017). Effect of electrode potentials on the microbial community of photo bioelectrochemical systems. *World Journal of Microbiology and Biotechnology*, *33*, 149–156. https://doi.org/10.1007/s11274-017-2312-8

Xiao, Y., Wu, S., & Yang, Z. (2013). Isolation and Identification of electrochemically active microorganisms. *Progress in Chemistry*, *25*, 1771–1780.

Xiao, Y., Zheng, Y., Wu, S., Yang, Z. H., & Zhao, F. (2016). Nitrogen recovery from wastewater using microbial fuel cells. *Frontiers of Environmental Science and Engineering*, *10*, 185–191. https://doi.org/10.1007/s11783-014-0730-5

Yates, M. D., Kiely, P. D., Call, D. F., Rismani-Yazdi, H., Bibby, K., Peccia, J., … Logan, B. E. (2012). Convergent development of anodic bacterial communities in microbial fuel cells. *ISME Journal*, *6*(11), 2002–2013. https://doi.org/10.1038/ismej.2012.42

Yokoyama, H., Ishida, M., & Yamashita, T. (2016). Comparison of anodic community in microbial fuel cells with iron oxide-reducing community. *Journal of Microbiology and Biotechnology*, *26*, 757–762. https://doi.org/10.4014/jmb.1510.10037

Zhan, G., Zhang, L., Li, D., Su, W., Tao, Y., & Qian, J. (2012). Autotrophic nitrogen removal from ammonium at low applied voltage in a single-compartment microbial electrolysis cell. *Bioresource Technology*, *116*, 271–277. https://doi.org/10.1016/j.biortech.2012.02.131

Zhang, L., He, W., Yang, J. U., Sun, J., Li, H., Han, B., … Liu, S. (2018). Bread-derived 3D macroporous carbon foams as high performance freestanding anode in microbial fuel cells. *Biosensors and Bioelectronics*, *122*, 217–223. https://doi.org/10.1016/j.bios.2018.09.005

Zhang, Y. P., Chen, X., Yuan, Y., Lu, X. W., Yang, Z. Y., Wang, Y. J., & Sun, J. (2018). Long-term effect of carbon nanotubes on electrochemical properties and microbial community of electrochemically active biofilms in microbial fuel cells. *International Journal of Hydrogen Energy*, *43*, 16240–16247. https://doi.org/10.1016/j.ijhydene.2018.06.144

Zhang, Y. F., Min, B., Huang, L. P., & Angelidaki, I. (2011). Electricity generation and microbial community response to substrate changes in microbial fuel cell. *Bioresource Technology*, *102*, 1166–1173. https://doi.org/10.1016/j.biortech.2010.09.044

Zhao, F., Rahunen, N., Varcoe, J. R., Chandra, A., Avignone-Rossa, C., Thumser, A. E., & Slade, R. C. T. (2008). Activated carbon cloth as anode for sulfate removal in a microbial fuel cell. *Environmental Science and Technology*, *42*, 4971–4976. https://doi.org/10.1021/es8003766

Zhao, J., Wang, L., Tang, L., Ren, R., You, W., Farooq, R., … Zhang, Y. (2019). Changes in bacterial community structure and humic acid composition in response to enhanced extracellular electron transfer process in coastal sediment. *Archives of Mircobiology*, *201*, 897–906. https://doi.org/10.1007/s00203-019-01659-3

Zhao, S., Li, Y., Yin, H., Liu, Z., Luan, E., Zhao, F., … Liu, S. (2015). Three-dimensional graphene/Pt nanoparticle composites as freestanding anode for enhancing performance of microbial fuel cells. *Science Advances*, *1*, e1500372. https://doi.org/10.1126/sciadv.1500372